Valence Correlation Schemes and New Signatures of Nuclear Structure: A Simple Global Phenomenology for $B(E2{:}2_1^+ \rightarrow 0_1^+)$ Values

R. F. Casten[1] and N. V. Zamfir[1],[2],[3]

[1]*Brookhaven National Laboratory, Upton, New York 11973*
[2]*Clark University, Worcester, Massachusetts 01610*
[3]*Institute of Atomic Physics, Bucharest, Romania*

(Received 18 November 1992)

It is shown that a simple renormalization allows nearly all $B(E2{:}2_1^+ \rightarrow 0_1^+)$ values to be encompassed in a tight correlation envelope when plotted against N_pN_n. Through such a valence correlation scheme, "deviant" nuclei are highlighted, and it is concluded that $B(E2{:}2_1^+ \rightarrow 0_1^+)$ values alone can provide signatures, not only of quadrupole collectivity, but also of axial asymmetry, hexadecapole shapes, shape coexistence, saturation of collectivity, shell structure, and the evolution of shell gaps. Moreover, combined with $E(4_1^+)/E(2_1^+)$ ratios, $B(E2{:}2_1^+ \rightarrow 0_1^+)$ values provide a simple new signature to distinguish the two principal classes of nuclear phase transitions.

PACS numbers: 23.20.Lv

Nuclear physics is endowed with a rich array of data on hundreds of nuclei. Often, though, the phenomenology of particular observables [see Fig. 1(a)] is daunting in its complexity and, partly as a consequence, much of these data have never been fully assimilated or digested. However, the development of valence correlation schemes (VCSs) has altered this situation, allowing large quantities of data to be correlated in a rather simple fashion. A VCS is an approach that attempts to account for the systematic behavior of nuclear observables in terms of a simple dependence on the numbers of valence nucleons. VCSs are generally motivated by a microscopic ansatz concerning the key factors controlling the empirical phenomenology. One such VCS is the N_pN_n scheme [1] which correlates the behavior of many mean field observables [such as $E(2_1^+), E(4_1^+)/E(2_1^+)$, $B(E2{:}2_1^+ \rightarrow 0_1^+)$] in each region of medium and heavy nuclei. Other VCSs are applicable to intrinsic excitations, such as an interpretation [2] of 3_1^- states in terms of N_p+N_n. VCSs are useful in themselves, as aids in predicting properties of unknown nuclei, as pointers to the underlying interactions that dominate the evolution of structure, and in highlighting nuclei that deviate from the expected patterns.

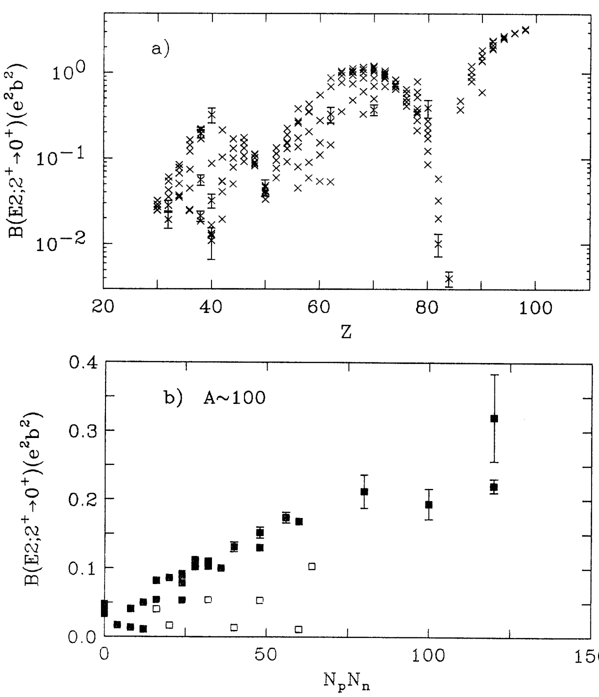

FIG. 1. (a) $B(E2{:}2_1^+ \rightarrow 0_1^+)$ values from Ref. [3] (published values) for $Z \geq 30$, plotted against Z. Error bars are shown if they exceed the size of the points. (b) $B(E2{:}2_1^+ \rightarrow 0_1^+)$ values for the $A \sim 100$ region plotted against N_pN_n. The open square symbols are *not* part of the main plot; they only illustrate where the Zr and Mo data points for $N<60$ *would* lie, if the $Z=38$ shell gap were ignored in counting N_p.

The purpose of this Letter is, first, to explore a remarkable VCS for $B(E2{:}2_1^+ \rightarrow 0_1^+)$ values that accounts for their phenomenology, not only in individual regions, but over *nearly the entire body of known nuclei*, and, second, to show that this VCS allows other degrees of freedom to be recognized solely from measured $B(E2{:}2_1^+ \rightarrow 0_1^+)$ values: That is, contrary to existing thought, $B(E2{:}2_1^+ \rightarrow 0_1^+)$ values are *not* merely an indicator of quadrupole collectivity and deformation (β_2), but also can give information on concepts such as axial asymmetry, hexadecapole deformation, shape coexistence, the nature of phase/shape transition regions, the saturation of collectivity, and shell structure and shell gaps and their evolution with N and Z—all this *without* the need to measure much more difficult observables [energies, $B(E2)$ values, moments] involving higher lying intrinsic states. This VCS facilitates predictions for unknown nuclei and presents a challenge to microscopic theory.

Published $B(E2{:}2_1^+ \rightarrow 0_1^+)$ [henceforth $B(E2)$] values compiled in Ref. [3] are plotted against Z for all nuclei with $Z \geq 30$ in Fig. 1(a). The complexity is obvious and the $B(E2)$ values span up to 3 orders of magnitude (hence the need for a log scale).

© 1993 The American Physical Society

As noted, the N_pN_n scheme correlates data very well in individual mass regions. This is illustrated in Fig. 1(b) for the $A=100$ region which shows a nearly linear dependence on N_pN_n. This region nicely exemplifies one application of VCSs mentioned above, namely, as indicators of shell gaps and their evolution. Figure 1(b) is obtained by assuming (in counting N_p) that $Z=38$ marks a shell gap for $N<60$. If this were not done, the data points for a number of nuclei (Zr, Mo, $N<60$) would deviate strongly from the trends established by the others. This point is demonstrated by the open squares in Fig. 1(b) which are plotted assuming that the proton shell is $Z=28$–50 (i.e., that $Z=38$ is not a shell gap). Clearly they lie far from the correlation envelope of the other points. The evolution of single-particle energies, and hence gaps, depends primarily on the monopole p-n interaction, and hence such plots give valuable information on such residual interactions. It is interesting to also note, given the current interest in radioactive beams, that evidence for or against double magicity in ^{100}Sn will probably be obtainable, by exploiting VCS plots such as Fig. 1(b), from Coulomb excitation of more readily available unstable nuclei in the mass region $A\sim100$–110 (e.g., Pd, Cd, Sn isotopes with $N\sim54$) long before ^{100}Sn itself is reached. Indeed, existing $B(E2)$ values in $^{102,104,106}Pd$ and $^{106,108,110}Cd$ already suggest, in the context of the VCS of Fig. 1(b), that $N,Z=50$ are magic when $N\gtrsim58$. Since shell gaps are evolutionary [4], this suggests, but of course does not assure, that ^{100}Sn is doubly magic.

We now tackle the more ambitious question of whether one can construct a global VCS for $B(E2)$ values, comparable to Fig. 1(b), but for nearly all known nuclei. Figure 2(a) plots the same $B(E2)$ values as in Fig. 1(a) but against N_pN_n and shows obvious correlations but also several distinct branches. The $E2$ operator, r^2Y_{20}, has a radial dependence which varies with nuclear size (N,Z). The Weisskopf unit (W.u.) incorporates this. Since we are comparing such disparate nuclei as Se and Pu, it is worthwhile to express the $B(E2)$ values in W.u. instead of the absolute units e^2b^2. Figure 2(b) does this and shows additional simplification but distinct families persist (see also Ref. [5]). Detailed inspection suggests a residual A or Z dependence. To incorporate this, we plot in Fig. 3(a) the same $B(E2)$ values (in W.u.) but now divided by A.

Though perhaps not evident at first glance (but see below), Fig. 3(a) shows that, of the ~200 values, almost 90% actually lie on a very tightly correlated path against N_pN_n and that there are about 20 "deviant" nuclei [highlighted in Fig. 3(a)], comprising the $A\sim180$ region (Hf–Os), lying well below the main sequence, and the

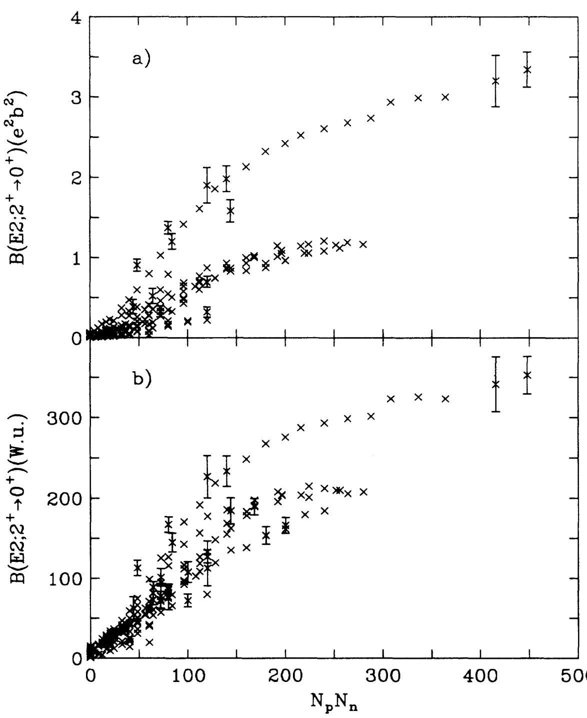

FIG. 2. The $B(E2)$ values of Fig. 1(a), plotted against N_pN_n (a) in e^2b^2 and (b) in W.u.

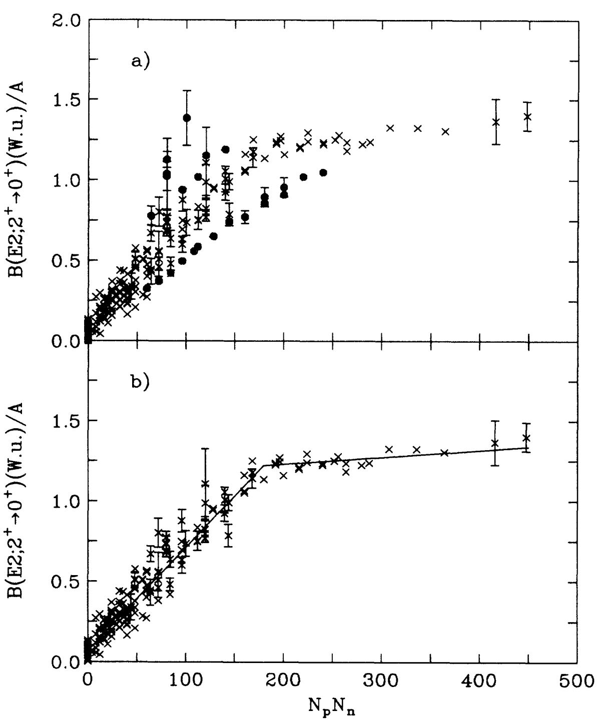

FIG. 3. $B(E2)$ values in W.u. divided by mass number A. (a) For the same nuclei as Fig. 1(a) and Fig. 2. Some data points for nuclei deviating from the main sequence are shown as solid circles. (b) Excluding the few deviant points. This plot includes a bilinear fit of the form $B(E2)=a+bN_pN_n$, where $a=0.07$, $b=0.0065$ W.u./A for $N_pN_n<175$, and $a=1.14$, $b=0.0004$ W.u./A for $N_pN_n>175$.

$N = 90,92$ isotopes of Sm and Gd and five Kr and Sr nuclei near $A = 76$ that lie above. None of these stand out in normal plots or even in Fig. 2.

We will return to these deviant nuclei later, but, for now, it is useful to simply remove them from the plot. The result, which is the goal of this process, is Fig. 3(b), which shows a remarkably well correlated sequence of $[B(E2)\ (\mathrm{W.u.})]/A$ values in which virtually all points trend upward in a compact envelope against N_pN_n. If nuclei with Z down to Mg are included, the correlation envelope broadens somewhat at the base but remains intact. The trend in Fig. 3(b) is exactly linear up to $N_pN_n \approx 180$, reflecting the growth of collectivity as valence neutrons and protons are added. For $N_pN_n \gtrsim 180$, there is a distinct break and the initiation of another, flatter, linear segment corresponding to a *saturation region*, where the addition of further valence nucleons hardly increases the collectivity. This remarkably compact phenomenology can be easily fit with a bilinear function, as shown. The 1σ deviation is $\pm 23\%$, and 2σ corresponds to a $\pm 50\%$ range. This is to be compared with the nearly 3 orders of magnitude spread in Fig. 1(a). Note that the success of this VCS provides a guide to the prediction of $B(E2)$ values for unknown nuclei since, in contrast to the *extrapolation* necessary for such nuclei in plots against N, Z, or A, predictions are often obtained by *interpolation* in the N_pN_n scheme.

This $B(E2)/A$ vs N_pN_n VCS, of obvious interest in itself for the remarkable correlation obtained, is also useful in identifying, highlighting, and elucidating the structure of nuclei that deviate from it. It is indeed just these nuclei that are known to possess anomalous shapes. The Sm-Gd and $A = 180$ groups are the principal nuclei below Pb known to have large β_4 deformations, positive and negative β_4, respectively [6]. In the liquid drop formulation the quadrupole moment can be expressed [7]

$$Q = K\beta_2[1 + 0.360\beta_2 + 0.967\beta_4]\,, \tag{1}$$

where K is a constant. Thus, the known signs of β_4 should lead to $B(E2)$ values ($\propto Q^2$) deviating from the VCS in just the directions observed in Fig. 3(a). The third group of deviant points in Fig. 3(a) are the anomalously high values for Sr-Kr nuclei. We will discuss these nuclei below.

First, we want to introduce another correlation involving $B(E2)$ values that may be of equal or greater consequence since it leads to a new signature for distinguishing the two major types of nuclear phase transitions.

Both $B(E2)$ values and the energy ratio $R_{4/2} = E(4_1^+)/E(2_1^+)$ are familiar indicators of structure. Since both observables increase with the onset of deformation and collectivity, one might think they would be simply correlated. However, Fig. 4(a) shows that this is decidedly *not* the case. While there is an overall trend, the correlation is poor: for a given $R_{4/2}$ value, $B(E2)$ values can vary by more than an order of magnitude. However, by exploiting the VCS of Fig. 3, we obtain a more revealing picture, shown in Fig. 4(b), which discloses two distinct tracks for $R_{4/2} \gtrsim 2.5$. One continues nearly linearly upwards to large $B(E2)$ values as $R_{4/2} \rightarrow 3.33$. The other, lower track is flatter at first, increasing sharply only for $R_{4/2}$ very close to 3.33.

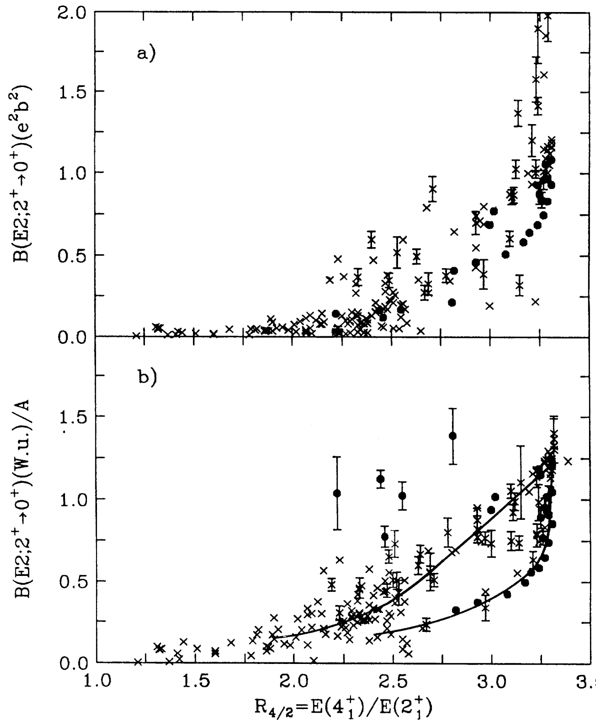

FIG. 4. Plot of $B(E2)$ values against $R_{4/2} = E(4_1^+)/E(2_1^+)$. (a) $B(E2)$ values in e^2b^2. (b) $B(E2)$ values in W.u., divided by A. The solid circles are the same nuclei as in Fig. 3. The curves for the two tracks are drawn to guide the eye.

There are two principal observed classes of nuclear phase transitions—spherical vibrator$\rightarrow$symmetric rotor and axially asymmetric (especially γ-soft)$\rightarrow$symmetric rotor. $R_{4/2}$ varies between roughly 2.3 and 3.33 in *both* cases and $B(E2)$ values also increase throughout both. The distinction between them is therefore difficult and often requires extensive data on higher-lying intrinsic excitations in sequences of nuclei. However, the two empirical tracks in Fig. 4(b) instantly provide a very simple new signature to classify phase transitions, obtainable from $B(E2)$ and $R_{4/2}$ values for even a single nucleus, when it is noted that the upper track consists of nuclei in spherical vibrator$\rightarrow$symmetric rotor transitional regions and the lower track corresponds to a γ-soft$\rightarrow$symmetric rotor transition region. The solid symbols along this lower track are from the well known $A \sim 180$ Hf-Os nuclei with large γ values, while those on the upper track, the Sm-Gd nuclei, are transitional from spherical vibrator to deformed rotor. We note in passing that the scatter near $R_{4/2} \sim 2.3$ reflects a range of anharmonicities in vibrational nuclei.

For γ values typical of the $A \sim 180$ region, the Davydov model [8] predicts a decrease in $B(E2)$ values. This decrease, in first order, is in addition to that from β_4. Together, the β_4-γ effect is roughly (20–25)%, not in bad accord with the values in Fig. 3(a), and with the fact that the $A \sim 180$ points in Fig. 3(a) are further from the VCS envelope [defined by Fig. 3(b)] than the Sm–Gd nuclei.

Finally, we return to the Sr–Kr nuclei, and note that they deviate from the trends in *both* Figs. 3(a) and 4(b) and are the *only* nuclei to do so. They are also perhaps the best known examples of strong prolate-oblate coexistence [9]. Mixing of an excited 0^+ band with a highly deformed ground-state band has been invoked [10] as an argument for a low $R_{4/2}$ value in these nuclei, since such mixing preferentially lowers the 0_1^+ state. However, Fig. 3(a) shows that, independent of the deviant $B(E2)$-$R_{4/2}$ correlation, the $B(E2)$ values themselves are much larger than expected. This may reflect unusually large deformations [11] but needs to be further investigated.

To summarize, we have shown that a plot of $[B(E2{:}2_1^+ \rightarrow 0_1^+)\ (\mathrm{W.u.})]/A$ against N_pN_n gives a VCS that accommodates *nearly all* $B(E2)$ values from light nuclei to the actinides in a single scheme amenable to a fit with a pair of linear expressions in N_pN_n. [In regard to theoretical interpretations of these results, we note that division by A is empirical and that almost identical results are obtained if the $B(E2)$ (W.u.) values are divided by Z, by (Z,A) combinations of the same order such as Z^2/A, or by powers differing from these by up to 1/6.] The correlation of $[B(E2{:}2_1^+ \rightarrow 0_1^+)\ (\mathrm{W.u.})]/A$ and $E(4_1^+)/E(2_1^+)$ was studied and found to be bivalued in transitional regions, providing a simple new signature to classify nuclear phase transitional regions. From these results it was shown that $B(E2{:}2_1^+ \rightarrow 0_1^+)$ values contain much more than information on quadrupole deformation alone and that they can give evidence on hexadecapole (β_4) deformations, axial asymmetry (γ), shape coexistence, the nature of nuclear phase transitions, shell structure and gaps, the saturation of collectivity, and can facilitate predictions for unknown nuclei by interpolation. With the advent of radioactive beam facilities, such tools will be valuable aids in deciphering structure and its evolution from a minimum of new data. Finally, any successful VCS, such as this, offers a challenge to microscopic theories. When the VCS encompasses nearly the whole chart of the nuclides, the challenge is both more demanding and compelling, and potentially more enlightening.

Work has been performed under Contracts No. DE-AC02-76CH00016 and No. DE-FG02-88ER40417 with the U.S. Department of Energy. We are grateful to B. R. Mottelson, W. Nazarewicz, D. S. Brenner, and W.-T. Chou for useful discussions.

[1] R. F. Casten, Nucl. Phys. **A443**, 1 (1985).
[2] N. V. Zamfir, R. F. Casten, and P. von Brentano, Phys. Lett. B **226**, 11 (1989).
[3] S. Raman *et al.*, At. Data Nucl. Data Tables **36**, 1 (1987).
[4] P. Federman and S. Pittel, Phys. Lett. **69B**, 385 (1977); **77B**, 29 (1978); R. F. Casten *et al.*, Phys. Rev. Lett. **47**, 1433 (1981).
[5] P. D. Cottle, Phys. Rev. C **43**, 1572 (1991).
[6] D. L. Hendrie *et al.*, Phys. Lett. **26B**, 127 (1968).
[7] F. K. McGowan *et al.*, Phys. Rev. Lett. **27**, 1741 (1971).
[8] A. S. Davydov and G. I. Filippov, Nucl. Phys. **8**, 237 (1958).
[9] R. B. Peircey *et al.*, Phys. Rev. Lett. **47**, 1514 (1981).
[10] M. Seiwert, A. V. Ramayya, and J. Maruhn, Phys. Rev. C **29**, 284 (1984).
[11] C. J. Lister *et al.*, Phys. Rev. Lett. **49**, 308 (1982).